

Discussions on Signal Uncertainty Principle in Shannon Channel Capacity

Equation and Research on Breaking Shannon Limit Method

Dequn Liang^{1*}, Xinyu Dou¹

Affiliations:

¹School of Information Science and Technology, Dalian Maritime University, Dalian, China

*Corresponding author. Email: ldqlgn@163.com

Abstract:

So far, the transmission rate of digital communication has approached the theoretical upper limit proposed by Shannon 70 years ago, and the academia and industry circles are puzzled by the lack of new theories to point out the direction of further increasing the transmission rate. In this paper, the completeness of Shannon channel capacity equation is analyzed in the framework of signal uncertainty principle, which brings the Shannon theory a more solid physical theoretical basis. Then the theoretical method of breaking through the Shannon Limit is proposed. Finally, it is proved that the time-shifted non-orthogonal multi-carrier digital modulation technology which we have studied for more than 20 years is a practical method to break through the Shannon Limit.

1. Introduction

The Intelligent devices are being deeply integrated with Internet through communication technologies, especially wireless communication technologies. The flexible, efficient and reliable information exchange between people and people, people and things, and even things and things will provide important supports for the upcoming new industrial revolution! This tendency also promotes the wireless communication technologies to 5G. The much higher data rate, higher spectral efficiency, and smaller delays or latency will be required for wireless communications^[1-3]. To achieve that goal, the industry has proposed a variety of technical solutions^[4-12]. Unfortunately, these technical solutions are on the direction of expanding the

usage of physical resources and improving prior arts, such as expanding spectrum resources, developing various new multi-user access technologies, signal processing techniques and coding methods. So far, the theoretical studies for breaking through Shannon limit are scarce. Shannon published two articles in 1948 and 1949 [13, 14], which laid a theoretical foundation of information processing and communication technologies. In these two articles, Shannon deduced the equation of channel capacity, indicating that there exists an upper limit of data transmission rate on a single physical channel with white noise (hereinafter referred to as the Shannon Limit), and pointed out that this upper limit could be infinitely approached with an arbitrarily small error rate by incorporating sufficiently involved (channel) encoding systems.

Since modern times, Shannon's information theory has been greatly developed and expanded in many fields. These extensions are mainly manifested in computer-centric information processing [21,22], including word processing, image recognition, language understanding, learning theory, social sciences and various other applications. However, looking back on the past, our research and understanding of Shannon's theory is not deep enough, so the communication industry generally believes that the data transmission rate has reached the upper limit! Therefore, the main evolution direction of the communication technology focusses on the information compression and channel coding, and the Shannon limit is still the upper limit of the data transmission rate. For instance, the LDPC and Polar coding, which have been included in the 5G standards, are just approaching rather than exceeding the Shannon limit [23,24]. 5G will further improve the transmission rate by greatly increasing the number of antennas to form a large-scale MIMO (multiple input and multiple output). The complexity and cost of deployment will be significantly increased. Although it has been proved that MIMO can break the Shannon limit, it is realized by synthesizing multiple physical channels through multiple antennas. The Shannon limit is still not broken through in a single physical channel [5,6,25-29]. In other words, the telecommunication theory is still based on the theory established by Shannon 70 years ago. This insufficiency of breakthrough in the basic theory makes some leaders and scholars of large telecommunication enterprises feel confused about

the further development of the telecommunication industry. Has the data transmission rate really reached its upper limit? In response to this issue, this paper introduces a method of waveform construction based on the time-delay overlapping principle, which makes it possible for breaking through the Shannon Limit.

2.The Shannon Channel Capacity Limit

In [13,14], based on the technical knowledge background in that era, and through large numbers of mathematical descriptions, Shannon introduced the statistical mechanics into the communication system to measure the uncertainty of information, which laid the foundation of the information theory. In this paper, the discussion is limited to Shannon's equation for transmitting the maximum average information on a continuous channel interfered by Gaussian white noise under the condition of constrained signal bandwidth and power. This equation is expressed as:

$$C = W \log_2 \frac{P + N}{N} = W \log_2 \left(1 + \frac{P}{N} \right) = W \log 2 (1 + SNR) \quad (1)$$

or

$$C/W = \log_2 \frac{P + N}{N} = \log_2 \left(1 + \frac{P}{N} \right) = \log 2 (1 + SNR) \quad (2)$$

where W is the signal bandwidth, P and N are the average power of the signal and the Gaussian white noise added to the channel, respectively, and the SNR represents the signal-to-noise ratio. Eq. (1) and Eq. (2) are respectively called Shannon channel capacity equation and transmission efficiency equation. The theoretical curve corresponding to Eq. (2) is plotted in Fig. 1, and two conclusions can be drawn as follows. Firstly, it is impossible to reach the upper region of the C/W curve, i.e., the C/W curve is the upper limit of the channel transmission efficiency (in bit/s/Hz). Secondly, this limit can be infinitely closed by sufficiently involved encoding systems with arbitrarily small frequency of errors. In order to better understand the breakthrough of the Shannon channel capacity equation, it is necessary to briefly introduce the derivation of the Shannon limit equation.

Shannon uses entropies to measure the statistical average information amount of both the discrete source and the continuous source. The entropy of the discrete source

is defined as:

$$H(X) = -\sum_{i=1}^M P(x_i) \log P(x_i) \quad (3)$$

where M is the number of discrete symbols contained in the message and $P(x_i)$ is the occurrence probability of the symbol x_i . For the continuous source, the continuation entropy is defined as:

$$H(X) = -\int_{-\infty}^{\infty} p(x) \log p(x) dx \quad (4)$$

where $p(x)$ is the probability density function of continuous distribution of random variables. Eq. (4) is the average amount of information carried by one sampling point. Mathematically, it is easy to prove that under the condition of limited signal power,

the condition that Eq. (4) gets the maximum value is $p(x) = \frac{1}{\sigma\sqrt{2\pi}} e^{-x^2/(2\sigma^2)}$, which

is called the best probability density distribution, where $\sigma^2 = P$, $\int_{-\infty}^{\infty} x^2 p(x) dx = \sigma^2$,

and $\int_{-\infty}^{\infty} p(x) dx = 1$.

Under the best probability density distribution condition, Shannon gave a series of expressions as follows.

Corresponding to the transmission signal x , the received signal is $y=x+n$, where n represents the noise. As a result, the entropy of the transmitted signal is:

$$H(X) = \log_2 \sigma\sqrt{2\pi} = \log_2 \sqrt{2\pi P} \quad (5)$$

The entropy of received signal is:

$$H(Y) = \log_2 \sqrt{2\pi(P+N)} \quad (6)$$

In addition, the conditional entropy is:

$$H(Y/X) = H(N) \quad (7)$$

Further, there is the average amount of mutual information corresponding to one sampling point

$$I(X;Y) = H(X) - H(X/Y) = H(Y) - H(Y/X) \quad (8)$$

According to the sampling theory, for a continuous signal with a bandwidth

limited to W , it can be fully expressed with $2TW$ discrete samples in the interval T . This also means that the interval between two sample points is $1/(2W)$. These sampling points are arranged in chronological order, and their amplitudes are the randomly distributed according to the Gauss distribution. Therefore, the sampling points can be represented as the following random vectors: $\hat{X} = [\hat{x}(t_j) | j=1, \dots, 2TW]$ where $\hat{x}(t_j)$ denotes the value of each sampling point, which is the continuous random variable. Since all the sampled values are independent with each other, the probability density function of each sampling point is identical.

For a continuous signal with the bandwidth W , the number of minimum sampling points is $2WT$, so the average mutual information amount for this continuous signal is:

$$I(\hat{X}; \hat{Y}) = [H(\hat{X}) - H(\hat{X}/\hat{Y})] \cdot 2W = [H(\hat{Y}) - H(\hat{Y}/\hat{X})] \cdot 2W \quad (9)$$

Under the best probability density distribution condition, Eq. (9) will be maximized:

$$C = \max [H(\hat{X}) - H(\hat{X}/\hat{Y})] \cdot 2W = \max [H(\hat{X}) - H(\hat{X}/\hat{Y})] \cdot 2W \quad (10)$$

Upon Eq. (4), Eq. (5) and Eq. (6), we can get Eq. (1) consequently.

Shannon also proposed a transmission scheme to reach this transmission rate limit, which mainly includes the following two points. Firstly, the transmitted signals must approximate, in statistical properties, a white noise. Secondly, the demodulation can be realized by using the least R.M.S. error principle, that is, by comparing the received signal one by one with the possible $M=2^s$ samples in the transmitted signals, the transmitted signal with the minimum root mean square error is taken as the demodulation signal. This scheme can be expressed as

$$\lim_{\varepsilon \rightarrow 0} \lim_{T \rightarrow \infty} \frac{\log M(\varepsilon, T)}{T} = W \log \frac{P+N}{N} \quad (11)$$

where ε is the frequency of error and T is the duration of the signal. This means that no matter how small ε is chosen, we can, by taking T sufficiently large, get the transmission rate as near as we wish to $TW \log(1+P/N)$ binary digits in the time T .

It is worth mentioning that, for Eq. (11), it is necessary to discuss the principle of signal uncertainty. This is precisely where previous studies have not been in-depth. The Eq. (11) has not been quoted or discussed in previous literatures concerning Shannon limit. Uncertainty principle is one of the most fundamental theorems in quantum mechanics, and the uncertainty principle is also valid in the field of signal processing [31-33]. Briefly, it is impossible to determine the spectrum bandwidth and the time duration of one signal accurately at the same time. According to Fourier analysis, the limited duration in time domain will result in an infinitely wide spectrum in frequency domain, and vice versa. Therefore, in practice, to approach the Shannon Limit is impossible, because in actual communication situation, the time duration of the transmitted signal is always limited, which acts against the requirement for “taking T sufficiently large” in Eq. (11). Meanwhile, the limited T must lead to an infinitely wide W in frequency domain, which again acts against the requirement for “narrow bandwidth W ”. Fortunately, in engineering implementation progress, the bandwidth can be limited under the condition of a given frequency of error which is noted as ε in Eq. (11). For this purpose, various definitions for bandwidth are proposed, such as 3dB bandwidth, spectrum zero bandwidth, minimum fading bandwidth, etc. Furthermore, Shannon proposed the channel coding theory to realize $\varepsilon=0$, which makes Shannon's theory satisfy mathematical completeness.

According to Shannon's method to realize the maximum data transmission rate, the simulation program is designed, and the simulation result is shown in Fig. 1(d). The theoretical curve corresponding to Eq. (2) is also shown to verify the simulation results. In order to save space, the simulation program is omitted, but the main parameters involved in the simulation program are described as follows.

The power spectral density (PSD) of the narrowband Gaussian white noise and the signal in white noise form are denoted as n_0 and n_{si} , respectively, and n_{si}/n_0 denotes the signal to noise ratio (SNR). When n_{si} is changed with $i=1, \dots, L$ while n_0 keeps in constant, different SNRs can be obtained. Meanwhile, the bandwidth of signal and noise are both set as W (50 kHz in the simulation), so we have

$P_0 = \sigma_0^2 = Wn_0$ and $P_{si} = \sigma_{si}^2 = Wn_{si}$. As a result, the corresponding noise with power P_0 and the variance σ_0^2 , and the signal with the power P_{si} (1W in the simulation) and the variance σ_{si}^2 in time domain can be easily generated using MATLAB, as shown in Fig. 1(a) and (b). In addition, in the simulation, the transmitted signal $x(t)$, the noise $n(t)$, and the received signal $y(t)=x(t)+n(t)$ are represented by the discrete form $x(t_i)$, $n(t_i)$, and $y(t_i)=x(t_i)+n(t_i)$, according to the sampling theory, where $i=1,\dots,2TW$, and T is the time duration. Therefore, if each symbol represents s bits, there may be $M=2^s$ values for each $x(t_i)$. Obviously, the T is impossible to be infinite in the simulation, so in order to make the simulation results closer to Eq. (11), the above process must be repeated many times. The demodulation process is shown in Fig. 1(c), and the channel capacity under different SNR are shown in Fig. 1(d). We can see that except for some fluctuation induced by the white noise, the simulation result (blue curve) and the theoretical curve (red curve) are identical, which means that the simulation progress is correct.

We use the above section to repeat Shannon's derivation of channel capacity equation with the following three purposes:

(1) Preparing for the breakthroughs in Shannon Channel Capacity Equation in the following section;

(2) The idea of the principle of signal uncertainty embodied in Eq. (11) is demonstrated. This should not be neglected in the study of Shannon's theory. Without $T \rightarrow \infty$, there will be no “limited” sampling points, and without $\varepsilon \rightarrow 0$, there will be no “sufficiently involved” encoding system to reach the Shannon limit. Thus, without signal uncertainty theory, Shannon's equation lacks mathematical completeness.

(3) 2018 and 2019 mark the 70th anniversary of the publication of Shannon's two classic articles [13,14]. We intend to take this opportunity to recall the great contributions of Shannon. Firstly, measuring information capacity with “entropy”, which is the definition of uncertainty in thermodynamics, is a further development. The German physicist Clausius firstly used entropy to describe the rate of change of heat input to temperature in 1865 [34]. Boltzmann put forward the statistical physics

explanation of entropy in 1877 [35]. However, it was not until Shannon used entropy to measure information that people really realized that entropy was a measure of system disorder, and Jaynes (1957) regarded thermodynamic entropy as an application of Shannon's information theory [36]. The signal uncertainty principle shown in Eq. (11) is actually a representation of the uncertainty principle in quantum mechanics. With the development of astrophysics, microphysics and information technology, Heisenberg put forward the uncertainty principle in 1927, which shows its universality more and more [37]. Information theory is no longer limited to engineering theory in the field of communication, but gradually formed into a basic theory which has solid mathematical support and can be applied in many disciplines.

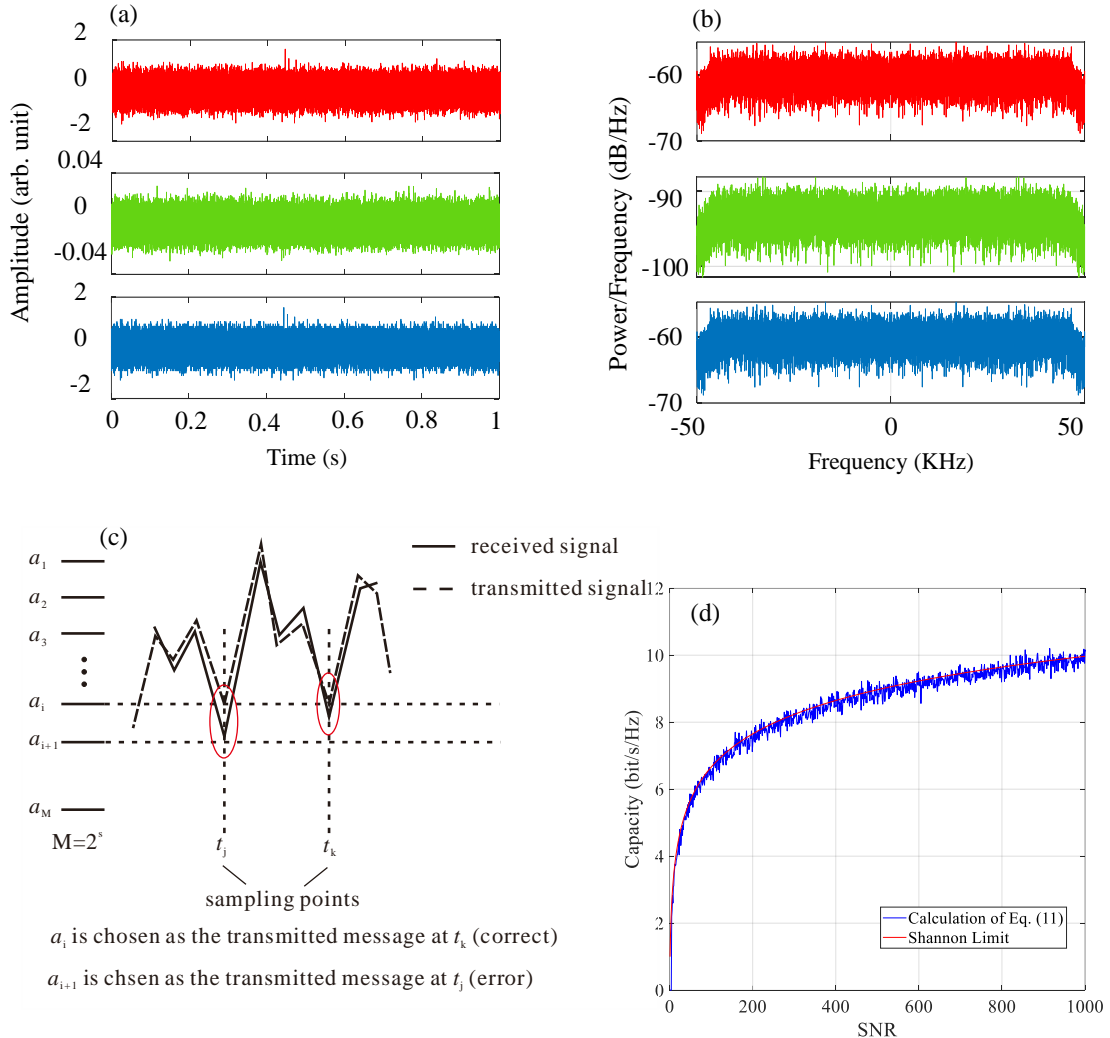


Fig. 1. Simulation results of the Shannon channel capacity limit. (a) Time domain waveform of the transmitted signal (top, red), Gaussian white noise (middle, green)

and the received signal (bottom, blue). (b) The PSD of the transmitted signal (top, red), Gaussian white noise (middle, green) and the received signal (bottom, blue). (c) Demodulation process described by Shannon. (d) Simulation results of the channel capacity (blue) and the theoretical calculation of Eq. (2) (red).

3. Derivation of the equation of Breaking Through Shannon Limit

There are two continuous random signals $\hat{x}_1(t_j)$ and $\hat{x}_2(t_j - \tau)$ which have the same bandwidth (noted as W) and the same average power (noted as P_1 and P_2) as well as the same probability density with normal distribution (σ^2 and ns represent respectively the mean square deviation and the probability density). This indicates that compared with $\hat{x}_1(t_j)$, the starting point of $\hat{x}_2(t_j - \tau)$ is delayed by $\hat{\tau}$ in time domain. Then each signal has $2TW$ samples based on the sampling theory and all the samples are the random variables with the same probability density of Gaussian distribution and the interval between adjacent sampling points is $1/(2W)$. These sampling values can be constructed as two random vectors $\hat{X}_1 = [\hat{x}_1(t_j), j = 1, \dots, 2TW]$ and $\hat{X}_2 = [\hat{x}_2(t_j - \hat{\tau}), j = 1, \dots, 2TW]$.

Obviously, \hat{X}_1 and \hat{X}_2 are independent of each other, so the amount of mutual information is $I(\hat{X}_1; \hat{X}_2) = 0$. Since their components have the same probability density there is $H(\hat{X}_1) = H(\hat{X}_2)$. Further, there is:

$$H(\hat{X}_1, \hat{X}_2) = H(\hat{X}_1) + H(\hat{X}_2) - I(\hat{X}_1; \hat{X}_2) = H(\hat{X}_1) + H(\hat{X}_2) = 2H(\hat{X}_1) \quad (12)$$

Specifying $\hat{\tau} = \frac{1}{2} \frac{1}{2W}$, the synthetic signal in the transmitter can be instructed as:

$$\hat{x}_0(t_i) = \hat{x}_1(t_{2j+1}) + \hat{x}_2(t_{2j}), i = 1, \dots, 4W, j = 0, 1, \dots, 2W - 1 \quad (13)$$

where $\hat{x}_1(t_{4TW})$ and $\hat{x}_2(t_0)$ are undefined (where $\hat{x}_1(t_{4TW}) = \hat{x}_2(t_0) = 0$). In fact, this is a process of forming a synthetic signal by inserting the samples of the second signal into the sampling intervals of the first signal in turn, thus this synthetic signal contains $4TW$ samples which are also independent with each other and have the same

normal distribution. There are the random vectors as $\hat{X}_0 = [\hat{x}_0(t_i) | i=1, \dots, 4TW]$, $\hat{X}_2 = [\hat{x}_2(t_{2j}) | j=1, \dots, 2TW]$, and $\hat{X}_0 = \hat{X}_1 + \hat{X}_2$.

In order to guarantee the average power constraint, the average power of the synthetic signal should be required to be equal to the average power of a single signal in Eq. (11). That is, $\|\hat{X}_0\|^2 = \|\hat{X}\|^2$ is required, where \hat{X} is the random vector in Eq. (9). According to the inner product theorem, there are $\|\hat{X}\|^2 = \langle (\hat{x}_1(t_i), \hat{x}_2(t_i)) | i=1, \dots, 2TW \rangle$ and $\|\hat{X}_0\|^2 = \langle (\hat{x}_0(t_i), \hat{x}_0(t_i)) | i=1, \dots, 4TW \rangle$. Due to the length of \hat{X}_0 is longer than that of \hat{X} , $\|\hat{X}_1\|^2 = \|\hat{X}_2\|^2 = \|\hat{X}\|^2/2$ is required.

This method of forming a synthetic wave is called as a delayed overlapping method.

Independent sampling points will generally be expanded and therefore overlap with each other after passing through the channel because of the low-pass or band-pass characteristics of the channel. If the signal is directly sampled at the receiver, the independence between the sampling point will be destroyed. However, suitable channel estimation and equilibrium methods can basically eliminate the expansion and overlapping of sampling points, and therefore restore the independence.

Thus, there is:

$$\hat{y}_0(t_i) = \hat{x}_0(t_i) + \hat{n}(t_i), i=1, \dots, 4TW \quad (14)$$

where $\hat{n}(t_i) = \begin{cases} n_1(t_{2i+1}) \\ n_2(t_{2i-\hat{\tau}}) \end{cases}, i=0, 1, \dots, 2TW$ is the noise item of the synthesized signal

at the receiver and there is a vector operation:

$$\hat{N} = \left\{ [n_1(t_{2i+1})]^2 + [n_2(t_{2i-\hat{\tau}})]^2 \right\} / 4TW = [n_0(t_{2i+1})]^2 / 2TW = N \quad (15)$$

where N is the noise average power in Eq. (10), and \hat{N} is the average power of $n(t_i)$ in Eq. (15).

According to Eq. (6), there is the conditional entropy $H(\hat{Y}_0 / \hat{X}_0) = H(\hat{N})$.

Corresponding to Eq. (14), there are the random vector $\hat{Y}_0 = [\hat{y}_0(t_i), i=1, \dots, 4TW]$ and the entropy $H(\hat{Y}_0)$.

According to the reciprocity principle in mathematics, \hat{X} and \hat{Y} in Eq. (9) can be replaced by \hat{X}_0 and \hat{Y}_0 , as a result, Eq. (9) can be converted to Eq. (16) as:

$$I(\hat{X}_0, \hat{Y}_0) = \left[H(\hat{Y}_0) - H\left(\frac{\hat{Y}_0}{\hat{X}_0}\right) \right] \cdot 4W \quad (16)$$

The maxima of Eq. (16), which represents the maximum channel capacity under the condition of two overlapping waves, can be obtained as:

$$\hat{C}_0 = \max I(\hat{X}_0, \hat{Y}_0) = \max \left[H(\hat{Y}_0) - H\left(\frac{\hat{Y}_0}{\hat{X}_0}\right) \right] \cdot 4W = 2W \log \frac{\hat{P}_0 + \hat{N}}{\hat{N}} = 2W \log \left(1 + \frac{\hat{P}_0}{2\hat{N}} \right) \quad (17)$$

By constructing a series of independent delay waveform $\hat{x}_1(t_j - \hat{\tau}_1)$, $\hat{x}_2(t_j - \hat{\tau}_2)$, ..., $\hat{x}_L(t_j - \hat{\tau}_L)$, the above derivation process is easily extended to the situation of L signals with independent and identically distribution, that is:

$$C_L = LW \log \left(1 + \frac{P + N}{LN} \right) = LW \log (1 + SNR/L) \quad (18)$$

or

$$C_L/W = L \log \left(1 + \frac{P + N}{LN} \right) = L \log (1 + SNR/L) \quad (19)$$

This is the equation to break through the Shannon limit. For the sake of distinction, we call the channel capacity equations described in Eq. (10) and Eq. (19) respectively as Shannon Capacity (ShC) and Time Delay Overlapping Shannon Capacity (OShC), respectively. The simulation results on the channel capacities corresponding to Eq. (19) under different conditions of $L=1$, $L=2$ and $L=5$ are shown in Fig. 2. As shown in Fig. 2, firstly, when L is larger than 1, the OShC is larger than ShC, which means that the Shannon limit can be broken through. Secondly, when L increases, the OShC is obviously enhanced, especially in positive SNR domain, which means that a large L , or a higher sampling rate, will lead to a higher channel capacity.

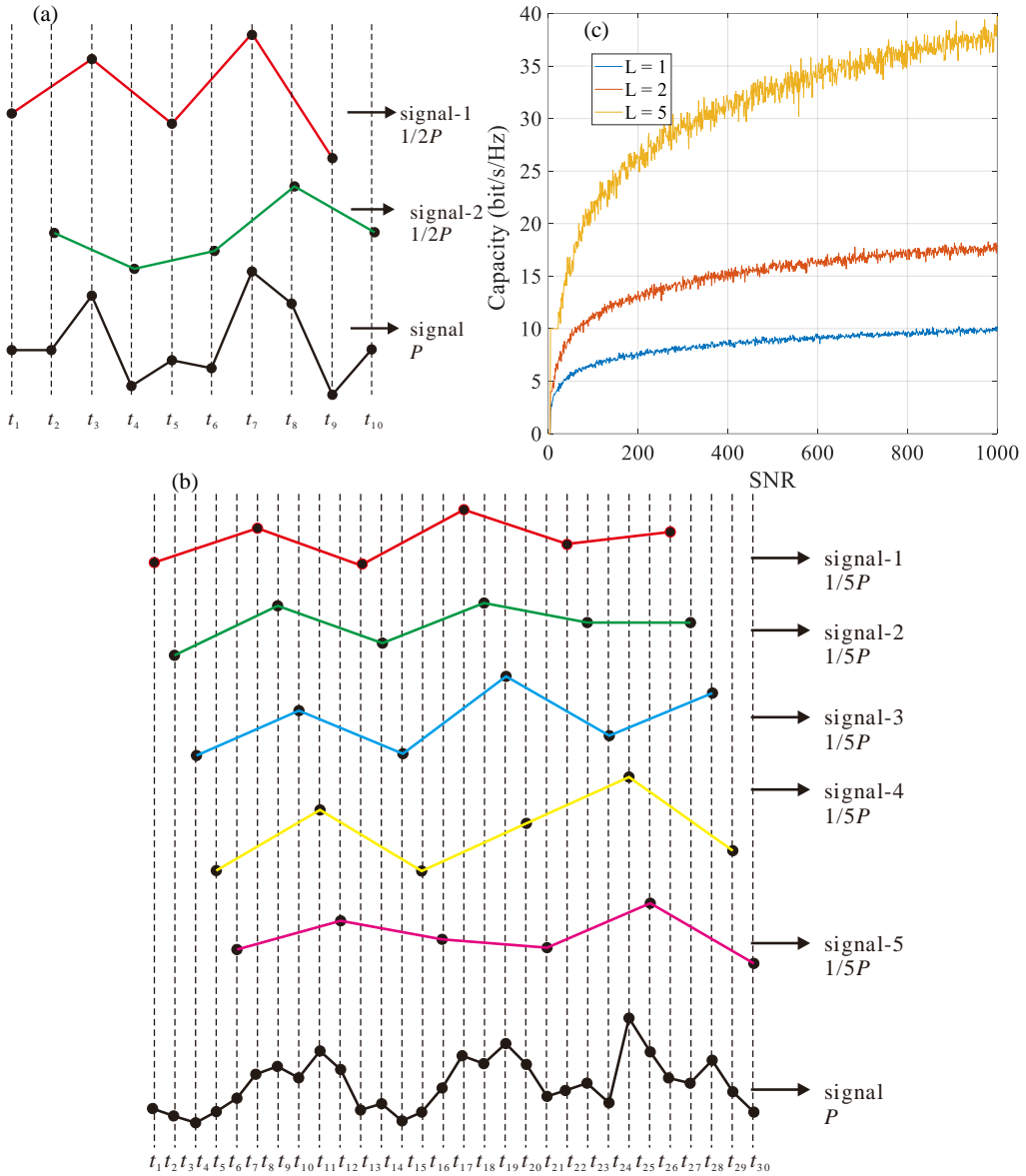


Fig. 2. Idea of time delay overlapping and the corresponding channel capacity. (a) Time delay overlapping by two independent signals. (b) Time delay overlapping by five independent signals. (c) The corresponding channel capacity. The blue, red and orange curve represents for the Shannon limit, time delay overlapping channel capacity under the condition of $L = 2$ and $L = 5$, respectively.

4. An Example of Modulation Techniques for Digital Communication Based on Time Delay Overlapping Method

In 1997, the author started to explore a more efficient modulation method for the digital communication. In 2000, the patent "phase shift overlapping code and

decoding method" (Patent No. H03M 13/37) was authorized, and then the author did not only a lot of relevant theoretical research, numerical simulation, and physics experiments, but also produced a number of new patents. Among them, the patent "Time-frequency-phase mixed multicarrier modulation method" (Patent No. H04L 27/26) embodies especially the idea of constructing efficient digital modulation by means of time-delay overlapping. After that we referred to this modulation technology as TS-NMT (Time-Shift Non-orthogonal Modulation Technology). In the process of studying TS-NMT, we gradually feel that the time-delay overlapping waveform construction method in TS-NMT can be used as a method to break through Shannon limit.

4.1 The waveform structures of the TS-NMT symbol

Firstly, we demonstrate the TS-NMT symbol forming process. A TS-NMT symbol is constituted by multiple base sub-carries. Each base sub-carrier can be sinusoidal (or cosinoidal) waves and has a duration T_d , which we define as lifetime. Outside the lifetime, the base sub-carrier equals to zero. To constitute the TS-NMT symbol, each base sub-carrier is time-delayed, amplitude modulated, and directly added in time domain. The whole process can be described as:

$$g(t) = \sum_{i=1}^8 a_i \sin \omega_i (t - \tau_i) \quad (19)$$

where $g(t)$ is the TS-NMT symbol, N is the number of base sub-carriers, $a_i \sin \omega_i (t - \tau_i)$ and τ_i are the i^{th} modulated base sub-carrier and the time-delay of the i^{th} base sub-carrier from the starting point of the symbol, respectively. A simple example is shown in Fig. 3. The TS-NMT symbol consists 8 modulated base sub-carriers, and all the angular frequencies are identical, i.e. $\omega_i = \omega_{i+1}$ ($i = 1, \dots, 8$). In practice, $\omega_i \neq \omega_{i+1}$ is also allowed. What's more, we set the time-delay interval between each base sub-carrier identical, and the duration of the TS-NMT symbol equals to approximately 2 times the lifetime of the base sub-carrier.

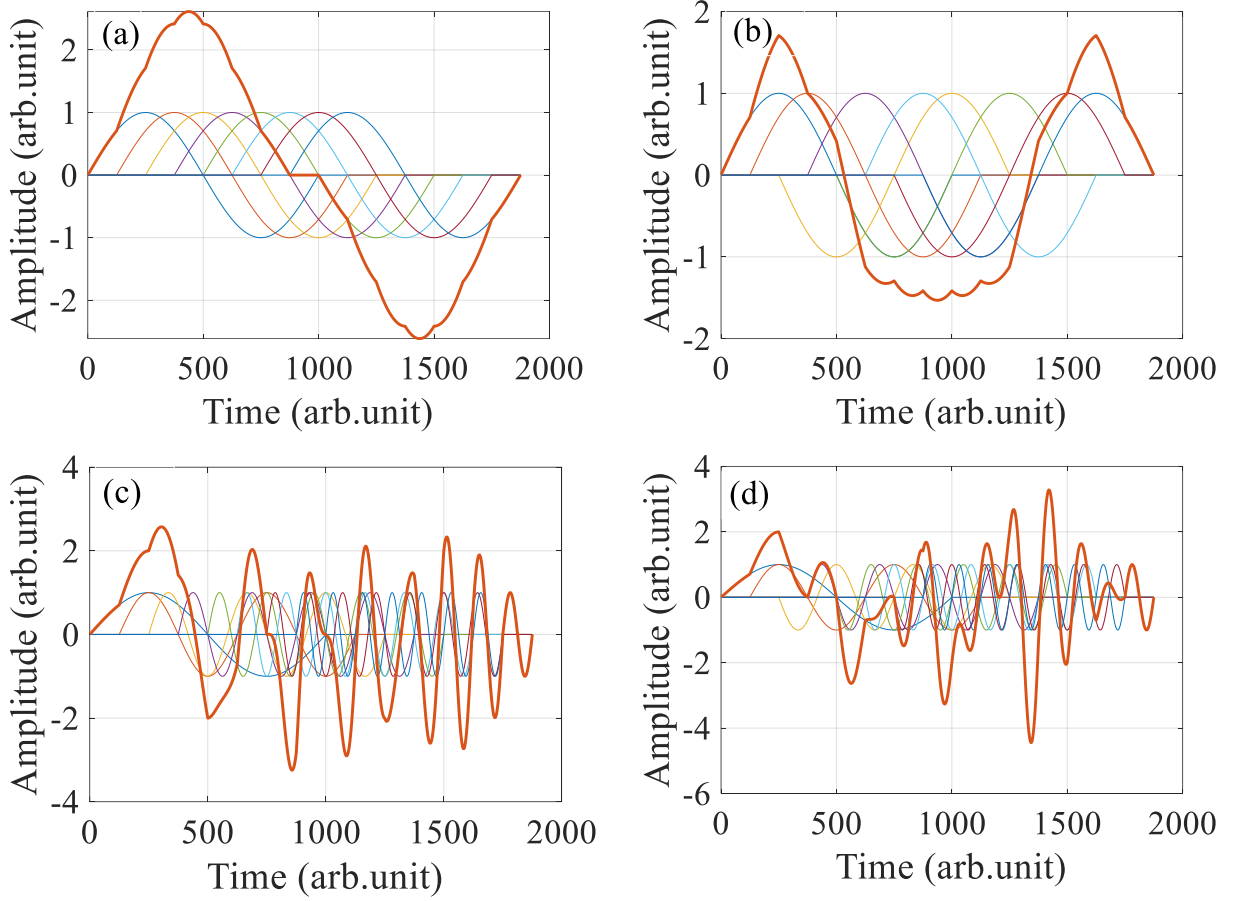


Fig. 3. Scheme of the symbol of TS-NMT. The colored curves and the bold curve represent for the base sub-carriers and the synthetic symbol waveform, respectively. (a) TS-NMT/S symbol carrying 8-bit +1 message by 8 subcarriers. (b) TS-NMT/S symbol carrying 8-bit message by 8 subcarriers (Each wavelet amplitude is randomly selected between 1 and-1). (c) TS-NMT/F carrying 8-bit +1 message by 8 subcarriers. (d) TS-NMT/F symbol carrying 8-bit message by 8 subcarriers (Each wavelet amplitude is randomly selected between 1 and-1).

More generally, the synthetic wave can be represented as:

$$g(t) = \sum_{i=1}^H a_i \bar{g} \omega_i(t_i - \tau_i), H \in T_{di} \quad (20)$$

where $\bar{g} \omega_i(t_i - \tau_i)$ are the base sub-carriers (their amplitudes are normalized), H is the number of the sub-carriers, and a_i is the amplitude of each sub-carrier. The value of ω_i is almost unlimited, except that the total bandwidth of the symbol does exceed

the specified value by the system. The base sub-carriers with the same angular frequency constitute one sub-channel in frequency domain.

Obviously, TS-NMT is a multi-carrier system like OFDM. All the sub-carriers and subchannels, however, are non-orthogonal to each other in the time and frequency domains. In the example illustrated in Fig.3 (a) and (b), there is only one sub-channel, so it is noted as TS-NMT/S, while the symbol containing multiple sub-channels is noted as TS-NMT/F, as shown in Fig. 3(c) and (d). The non-orthogonality of TS-NMT is one of the most important features different from OFDM.

The demodulation of TS-NMT cannot be realized by FFT used to OFDM due to the non-orthogonality. In this paper a demodulation method used by solving a system of linear equations has been proposed. The demodulation process includes two steps as below.

Step 1: A series of coherent operations are put in the order of delay τ_i ($i=1, \dots, H$) on the received symbol waveform in each symbol period, then a system of linear equations is obtained:

$$\mathbf{R}\mathbf{V}=\mathbf{B} \quad (21)$$

where \mathbf{R} is called as the demodulation matrix and is a Toeplitz matrix, and its elements are obtained by a series of the coherent operations as:

$$R = \int_{\tau_{ij}} \bar{g}_i(t_i - \tau_i) \bar{g}_j(t_j - \tau_j) dt = r_{ij}, i, j = 1, \dots, H \quad (22)$$

What's more, in Eq. (21), \mathbf{V} is called an amplitude vector waiting to be solved and is composed of the quantization amplitudes of the sub-carriers, and the vector \mathbf{B} is called as a coherent vector and is composed of the results of a series of coherent operations defined as follows,

$$B = \int_{\bar{T}} g_r(t) \bar{g} \omega_i(t_i - \tau_i) dt = b_i, i = 1, \dots, H \quad (23)$$

where $g_r(t)$ is the received symbol waveform.

Step 2: The amplitude vector \mathbf{V} of the received sub-carriers are obtained by resolving the equation group (21), that is, $\mathbf{V}=\mathbf{R}^{-1}\mathbf{B}$.

It should be noted that the subcarriers contained in a synthetic wave of the

TS-NMT are non-orthogonal, that is, the subcarrier vectors are non-orthogonal in the multi-dimensions linear space which is often called as the constellation in the digital communication, in which a star-point corresponds to an element of \mathbf{V} . We can construct an orthogonal constellation for OFDM, but for TS-NMT, we can only draw a two-dimension non-orthogonal constellation, as shown in Fig. 4(a). In OFDM the minimum distances between the star-points are equal, but in TS-NMT are not equal. However, each subcarrier can be projected onto the coordinate axis of each dimension by coherent operation, so each subcarrier can be solved separately on a one-dimensional constellation. In this way, the distance between the smallest star points is the same, and the independence between the subcarrier is guaranteed.

4.2 The analysis of the transmission efficiency of TS-NMT

The transmission efficiency is defined as $\eta_T = \text{bits}/S/W$ (S is Second and W is hertz). In [30] the theoretical analysis and computer simulation results of the comparison between TS-NMT and OFDM have been described in detail, and many of the advantages of TS-NMT relative to OFDM are introduced, such as the higher spectral efficiency, low peak average power ratio, higher anti frequency-shift ability, low power consumption, and so on.

The following description relates to the analysis of the possibility of TS-NMT as a practically available means of breaking through the Shannon Limit. Different from the literature [30], the following analysis is more focused on intuitive and qualitative description.

Firstly, the signal power of TS-NMT is demonstrated. In the traditional digital amplitude modulation method with noise, when the signal power is increased by 6 dB, the number of bits carried by the signal increases by one. According to that rule, if every subcarrier in Fig.3 (a) or (b) can carry one bit, the synthetic wave will carry eight bits, and therefore, the power of the synthetic wave will be increased by 48 dB than that of one subcarrier. However, an intuitive observation to the waveform structure in Fig. 3 shows that the power of the synthetic wave cannot be increased as that much. As can be seen from Figure 3 (b), in the time coordinate system, the phases of subcarriers are evenly distributed between 0 and 180 degrees in the interval

between 500 and 1500, which causes the amplitude of the synthetic wave to be less than the sum of the sampling values of the subcarriers due to the time-delay overlapping construction of the subcarriers. In fact, the simulation result is that the average power of the synthetic wave is only 7.4 dB larger than the average power of the single subcarrier. Thus, the power required for waveform transmission based on time-delay overlapping method is much less than that of the traditional method. We call it "power efficiency". The power efficiency of TS-NMT can be further explained by comparing TS-NMT with OFDM, as shown in Fig. 4(b). This further verifies the high power-efficiency of TS-NMT. Moreover, the theoretical analysis and computer simulation verification on the performance comparison between TS-NMT and OFDM are introduced in our previous research (30). In addition to the higher spectral efficiency than the OFDM, it also shows more advantages of TS-NMT, such as lower peak power mean ratio, higher anti frequency-shift ability, lower power consumption, and so on.

Then, the communication capacity and the communication performance of TS-NMT is shown in Fig. 4(c) and (d). It is worth noting that, since Shannon's channel capacity is deduced on the basis of continuous signals, we must verify that the TS-NMT signal belongs to the continuous signal. In Eq. (13) & Eq. (14), if $0 \leq t < T$ and $T \rightarrow \infty$ is defined, the waveform of TS-NMT belongs to the continuous waveform and can be tested by numerical simulation. In the simulation, the life-time and frequency of the sub-carrier is set as 1 s and 1 Hz, so the sub-carrier is one-period sinusoidal or cosine wave, as shown in Fig. 3(a) or Fig. 3(c). Under this condition, the time duration of the TS-NMT symbol is 2 s, and the null-to-null bandwidth is 2 Hz. From Fig. 4(c), we can see that the capacity of the TS-NMT system is higher than the Shannon Limit, especially for the higher SNR condition. The capacity of the TS-NMT system increases exponentially with the increasing of SNR. For each point in Fig. 4(c), the bit-error-rate (BER) is controlled to be less than 10^{-5} , and no channel coding is included in the system. Finally, the simulation results of the communication performance of TS-NMT are shown in Fig. 4(d). We can see that, for higher SNR condition, the capacity of the TS-NMT system will be more than 70 bit/s/Hz (the BER

is less than 10^{-5}). This means that for higher SNR condition, the capacity of the TS-NMT system will be far higher than the Shannon Limit.

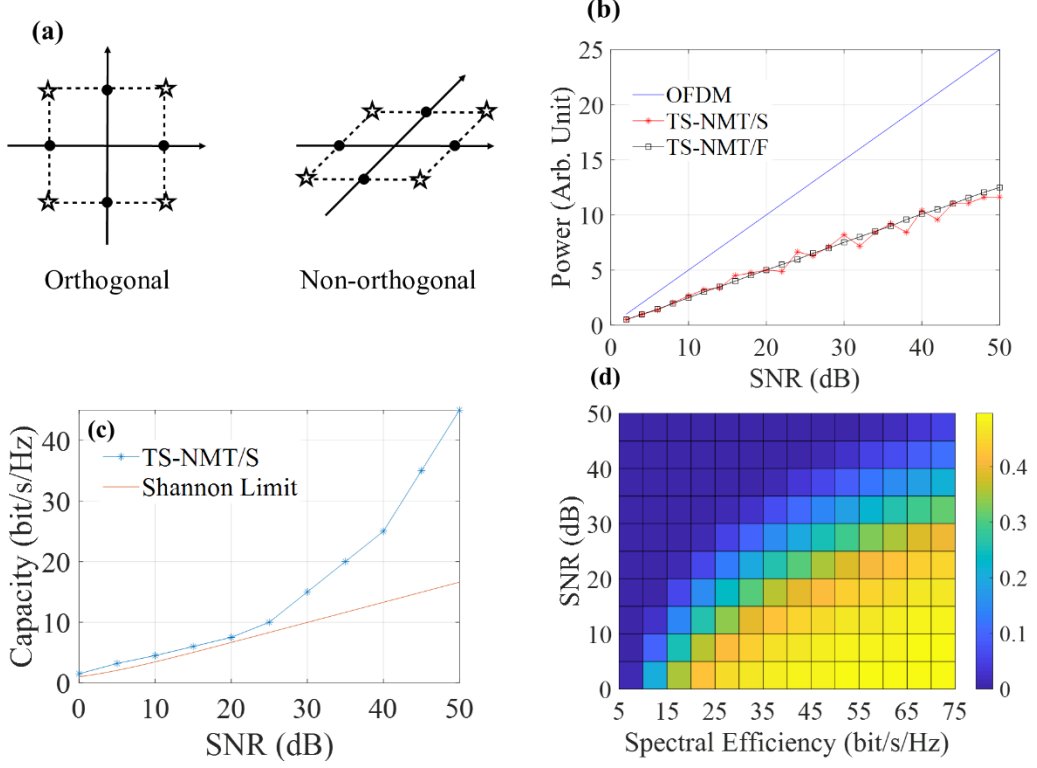


Fig. 4. Simulation results of TS-NMT. (a) Constellation of the orthogonal symbol and the non-orthogonal symbol. (b) Symbol power comparison between OFDM, TS-NMT/S and TS-NMT/F. (c) Channel capacities of TS-NMT/S comparing with the Shannon Limit. (d) BER performance of TS-NMT/S under different conditions.

4.3 Performance analysis of TS-NMT

In this section, we give some quantitative analysis on the communication performance of TS-NMT. From Eq. (21), the demodulation process of TS-NMT is the numerical solution of the equation set, and the numerical solution A is identified as the demodulation result of TS-NMT. As we all know that the numerical solution processes of the equation set will unavoidably encounter the ill-condition problem, i.e., the perturbation to the equation set will cause the deviation between the exact solution and the numerical solution. In other words, greater ill-condition will cause larger deviation between the exact solution and the numerical solution, and consequently, will cause higher bit error rate (BER) of the TS-NMT system. Thus, it is necessary to develop the origin of the ill-condition of equation set Eq. (21) and the methods to

mitigate or even eliminate the ill-condition problem.

For digital communication system, the direct perturbation on the communication signal is the Gaussian white noise and the filtering effect of the communication channel. Concerning these perturbations, equation set Eq. (21) will be

$$\mathbf{R}(\mathbf{A} + \Delta\mathbf{A}) = \mathbf{B} + \Delta\mathbf{B} \quad (24)$$

where $\Delta\mathbf{B}$ is the consequence of the above perturbation factor, and $\Delta\mathbf{A}$ represents for the deviation between the exact solution and the numerical solution, i.e., bigger $\Delta\mathbf{A}$ means higher BER of TS-NMT.

In TS-NMT, all the variables are quantified under some level of accuracy, and we have the identical equation

$$\mathbf{R}\mathbf{A} \equiv \mathbf{B} \quad (25)$$

According to Eq. (24) and Eq. (25), we have

$$\Delta\mathbf{A} = \mathbf{R}^{-1}\Delta\mathbf{B} \quad (26)$$

where \mathbf{R}^{-1} is the inverse matrix of \mathbf{R} . Because $\|\Delta\mathbf{A}\| \leq \|\mathbf{R}^{-1}\| \cdot \|\Delta\mathbf{B}\|$, we call $\|\mathbf{R}^{-1}\| \cdot \|\Delta\mathbf{B}\|$ the upper bound of $\|\Delta\mathbf{A}\|$. Obviously, lower $\|\mathbf{R}^{-1}\|$ brings lower $\|\Delta\mathbf{A}\|$, and lower BER will be obtained.

The ill-condition of TS-NMT can be decreased by adding an additional wave (a sharp downward spike for instance) in front of the sub-carrier waveform, as shown in Fig. 5. The amplitude, time-duration, position, and number of spikes are all the adjustable variables, and in Fig. 5 we set the time-duration of the spike be 1% of the life-time of the sub-carrier, and the amplitude of the spike be equal to that of the peak amplitude of the sub-carrier. Other TS-NMT symbol forming parameters are shown in Table 2. After adding the additional wave, the $\|\mathbf{R}^{-1}\|$ is reduced from 3.8465 to 0.0283, and the BER is reduced from 0.06 to less than 10^{-5} .

Table 1 TS-NMT symbol forming parameters

Parameter	Value
Type of the sub-carrier	Sinusoidal wave
Number of the sub-carrier	40

Interval of each sub-carrier (sampling points)	250
SNR (dB)	20
Amplitude of the additional wave	-1
Number of tested bits	10^6

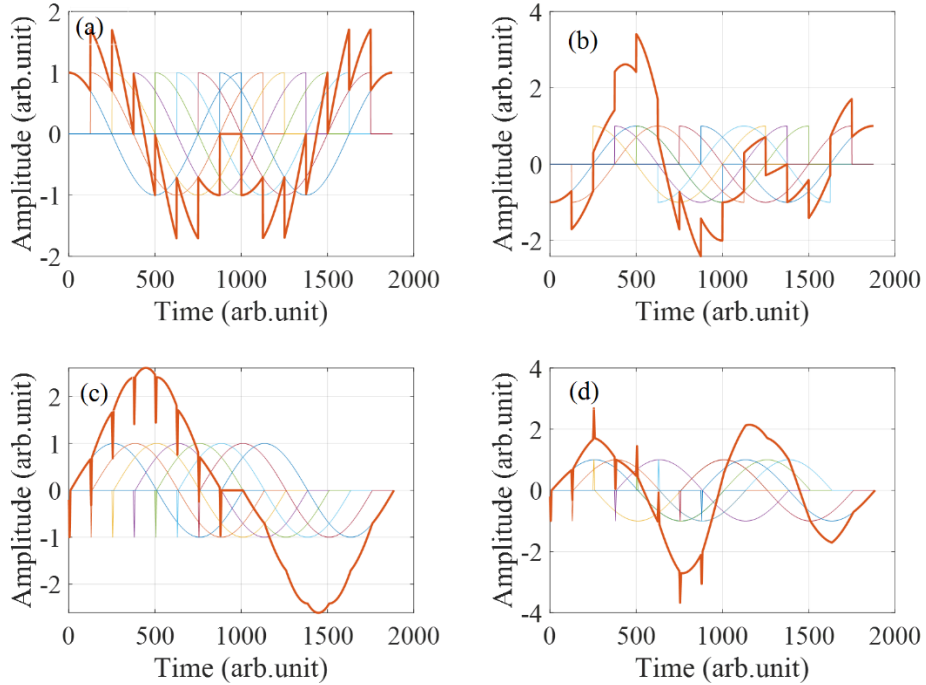


Fig. 5. Scheme of the TS-NMT symbol constituted by cosine sub-carriers or sinusoidal waves with additional waves. (a) TS-NMT symbol constituted by 8 cosine sub-carriers carrying 8 +1 signals. (b) TS-NMT symbol constituted by 8 cosine sub-carriers carrying 8 random “+1, -1”. (c) TS-NMT symbol constituted by 8 sinusoidal sub-carriers with additional wave carrying 8 +1 signals. (b) TS-NMT symbol constituted by 8 sinusoidal sub-carriers with additional wave carrying 8 random “+1, -1”.

The communication capacity and performance of the TS-NMT system with additional waves are shown in Fig. 6. Because the nonlinearity of the sub-carrier waveform is enhanced, the communication capacity of the system is further improved, especially for the cosine sub-carrier TS-NMT system, the communication capacity far exceeds the Shannon Limit. It is worth noting that, in Fig. 6, the TS-NMT system

belongs to TS-NMT/S system, where all the sub-carriers occupy only one frequency channel. If we simultaneously utilize multiple frequency channels, the capacity of the whole system will be multiplied. Thus, the TS-NMT technology can be considered as one of the practical methods to break through the Shannon Limit.

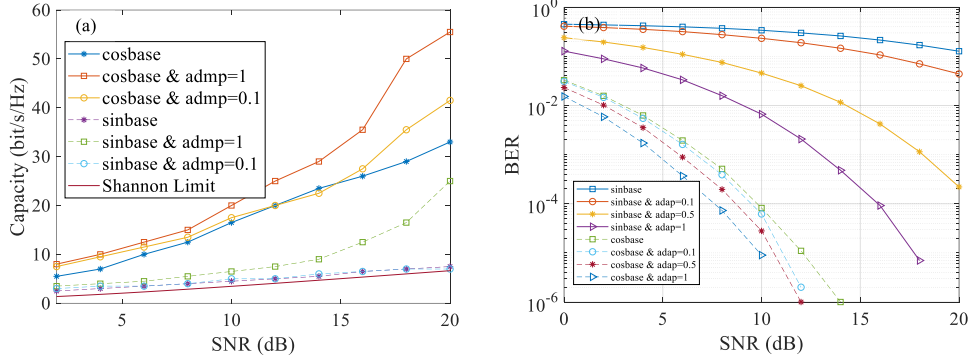


Fig. 6. Capacity and Performance of the TS-NMT system with additional waves. (a) Communication capacity. (b) Communication performance.

Nevertheless, we will face two problems as follows. Firstly, the property of the sinusoidal or cosine sub-carrier will be changed after adding the additional waves, and the \mathbf{R} in (21) will consequently be changed. That is to say, the subcarrier changes from $\sin(\omega(t-\tau_i))$ to $\sin(\omega(t-\tau_i))+p(t)$, where $p(t)$ represents the additional waves. However, because the TS-NMT is non-orthogonal, the sub-carriers forming \mathbf{R} in the coherent operation do not have to be standard sinusoidal or cosine waves. In fact, because the communication channel is always bandpass or lowpass channel, the sub-carriers in the received signal is also inevitably transformed. When we design a communication system, because the parameters are always known in priori (through estimation for instance), the transformed sub-carrier can be obtained through numerical training. The training process is demonstrated as follows,

$$s_r \omega(t-\tau_i) = s_t \omega(t-\tau_i) * h(t) * f(t) \quad (27)$$

where $s_t \omega(t-\tau_i)$ and $s_r \omega(t-\tau_i)$ are the transmitted and received base sub-carriers, respectively, $*$ is the convolution operation, $h(t)$ is the communication channel model, and $f(t)$ represents the filter.

Secondly, the higher frequency components in TS-NMT symbol spectrum will be enhanced by adding additional wave. However, through controlling the power of the additional spike and using appropriate filters, the higher frequency components will be neglected in the actual project.

Discussion

In more than 20 years of TS-NMT research, we have gradually realized that the time-delay overlapping method is an effective technical means to improve the transmission efficiency. For a long time, we have thought that this technology may break through the Shannon Limit. However, for the sake of caution, the above theoretical proof and simulation results have not been published until now. Thomas proved that independent multi-channel synthesis can linearly improve the efficiency of information transmission ^[21]. In fact, there is an intuitive understanding of the efficiency of TS-NMT. Firstly, a single physical channel is decomposed into several independent logical subchannels, and then the signals on these subchannels are reconstituted into synthetic waves by using time-delay overlapping method, which improves the efficiency of a single physical channel.

References

- [1] M. Shafi, A. F. Molisch, P. J. Smith, et al. 5G: A Tutorial Overview of Standards, Trials, Challenges, Deployment, and Practice. *IEEE Journal on Selected Areas in Communications*, vol. 35, no. 6, pp. 1201-1221, June 2017.
- [2] I. Parvez, A. Rahmati, I. Guvenc, et al. A Survey on Low Latency Towards 5G: RAN, Core Network and Caching Solutions. *IEEE Communications Surveys & Tutorials* (Early Access), 2018.
- [3] S. Buzzi, C. I, T. E. Klein, et al. A Survey of Energy-Efficient Techniques for 5G Networks and Challenges Ahead. *IEEE Journal on Selected Areas in Communications*, vol. 34, no.4, pp. 697-709, April 2016.
- [4] Z. Ding, Y. Liu, J. Choi, et al. Application of Non-Orthogonal Multiple Access in LTE and 5G Networks. *IEEE Communications Magazine*, vol. 55, no. 2, pp. 185-191,

Feb. 2017.

- [5] Y. Li, P. Fan, A. Leukhin, et al. On the Spectral and Energy Efficiency of Full-Duplex Small-Cell Wireless Systems With Massive MIMO. *IEEE Transactions on Vehicular Technology*, vol. 66, no. 3, pp. 2339-2353, Mar. 2017.
- [6] B. Ai, K. Guan, R. He, et al. On Indoor Millimeter Wave Massive MIMO Channels: Measurement and Simulation. *IEEE Journal on Selected Areas in Communications*, vol. 35, no.7, pp. 1678-1690, July 2017.
- [7] S. Chen, B. Ren, Q. Gao, et al. Pattern Division Multiple Access—A Novel Nonorthogonal Multiple Access for Fifth-Generation Radio Networks. *IEEE Transactions on Vehicular Technology*, vol. 66, no. 4, pp. 3185-3196, April 2017.
- [8] S. M. R. Islam, N. Avazov, O. A. Dobre, et al. Power-Domain Non-Orthogonal Multiple Access (NOMA) in 5G Systems: Potentials and Challenges. *IEEE Communications Surveys & Tutorials*, vol. 19, no. 2, pp. 721-742, Second Quarter 2017.
- [9] KNRSV Prasad, E. Hossain, and VK Bhargava. Energy Efficiency in Massive MIMO-Based 5G Networks: Opportunities and Challenges. *IEEE Wireless Communications*, vol. 24, no. 3, pp. 86-94, Jun. 2017.
- [10] B.P. Rimal, D. P. Van, and M. Maier. Mobile Edge Computing Empowered Fiber-Wireless Access Networks in the 5G Era. *IEEE Communications Magazine*, vol. 55, no. 2, pp. 192-200, Feb. 2017.
- [11] E. Baser. Index Modulation Techniques for 5G Wireless Networks. *IEEE Communications Magazine*, vol. 54, no.7, pp. 168-175, Jul. 2016.
- [12] Z. Ding, P. Fan, and H.V. Poor. Random Beamforming in Millimeter-Wave NOMA Networks. *IEEE Access*, vol. 5, pp. 7667-7681, 2017.
- [13] C. E. Shannon. A mathematical Theory of Communication. *Bell System Technical Journal*, vol. 27, no. 3, pp. 379-423, Jul. 1948.
- [14] C. E. Shannon. Communication in the Presence of Noise. *Proceedings of the I.R.E.* vol. 37, no. 1, pp. 10-21, Jan. 1949.
- [15] H. Kim. Coding and Modulation Techniques for High Spectral Efficiency Transmission in 5G and Satcom. *23RD EUROPEAN SIGNAL PROCESSING*

CONFERENCE (EUSIPCO), 2015.

- [16] S. Chen, K. Peng, Y. Zhang, et al. Near Capacity LDPC coded MU-BICM-ID for 5G. INTERNATIONAL WIRELESS COMMUNICATIONS & MOBILE COMPUTING CONFERENCE (IWCMC), 2015.
- [17] H. Gamage, N. Rajatheva, and M. Latva-Aho. Channel Coding for Enhanced Mobile Broadband Communication in 5G Systems. EUROPEAN CONFERENCE ON NETWORKS AND COMMUNICATIONS (EUCNC), 2017.
- [18] G. Durisi, T. Koch, and P. Popovski. Toward Massive, Ultrareliable, and Low-Latency Wireless Communication With Short Packets. Proceedings of the IEEE, vol. 104, no. 9, pp. 1711-1726, Sep. 2016.
- [19] L. Dong, H. Zhao, Y. Chen, et al. Introduction on IMT-2020 5G Trials in China. IEEE Journal on Selected Areas in Communications, vol. 35, no. 8, pp. 1849-1866, Aug. 2017.
- [20] J. Dai, K. Niu, Z. Si, et al. Polar Coded Non-Orthogonal Multiple Access. IEEE INTERNATIONAL SYMPOSIUM ON INFORMATION THEORY, 2016.
- [21] Cover, T.M. and Thomas, J.A. (1991) Elements of information theory. Wiley, New York.
- [22] M. Kelbert and Y. Suhov. (2013) Information Theory and Coding by Example. Cambridge University Press, UK.
- [23] F. Babich, A. Soranzo, and F. Vatta. Useful Mathematical Tools for Capacity Approaching Codes Design. IEEE Communication Letters, vol. 21, no. 9, pp. 1949-1952, Jun. 2017.
- [24] E. Pise, D. Pajan, S. Abu-Surra, et al. Capacity-Approaching TQC-LDPC Convolutional Codes Enabling Power-Efficient Decoders. IEEE Transactions on Communications, vol. 65, no. 1, pp. 1-13, Oct. 2016.
- [25] Telatar E. Capacity of multi-antenna Gaussian channels. European Transactions on Telecommunication, vol. 10, no. 6, pp. 585-596, 1999.
- [26] P. F. Driessen, G. J. Foschini. On the capacity formula for multiple input-multiple output wireless channels: a geometric interpretation. IEEE Transactions on Communications, vol. 47, no. 2, pp. 173-176, 1999.

[27]G. Gampala, and C. J. Reddy. Massive MIMO - Beyond 4G and a Basis for 5G. International Applied Computational Electromagnetics Society Symposium (ACES), 2018.

[28]X. Gao, L. Dai, S. Han, et al. Energy-Efficient Hybrid Analog and Digital Precoding for MmWave MIMO Systems with Large Antenna Arrays. IEEE Journal on Selected Areas in Communications, vol. 34, no. 4, pp. 998-1009, Apr. 2016.

[29]N. Liang and W. Zhang. Mixed-ADC Massive MIMO. IEEE Journal on Selected Areas in Communications, vol. 34, no. 4, pp. 983-97, Apr. 2016.

[30]Dequn Liang, Mingyan He, Qisheng Cao, Ganna Liu. A Multi-Carriers Modulation Technology with Higher Spectral Efficiency and Stronger Capability Tolerating the Frequency Shift, Intelligent Signal Processing and Communication Systems(ISPACS 2011), Chiangmai, Thailand, 7-9 December, 2011.

[31]Peng Wang, and Jianping Li. Quantum Interpretation of Signal's Uncertainty Principle. Journal of University of Electronic Science and Technology of China, vol. 37, no. 1, pp. 14-16, 2008.

[32]L. Cohen. (1995) Time-frequency Analysis Theory and Application. Prentice Hall, New York.

[33]M. Rosler, M. Voit. An Uncertainty Principle for Hankel Transforms. Proceedings of the American Mathematical Society, vol. 127, 1998.

[34]R. Clausius. (1865) The Mechanical Theory of Heat – with its Applications to the SteamEngine and to Physical Properties of Bodies. John van Voorst, London.

[35]L. Boltzmann. On the Relationship between the Second Fundamental Theorem of the Mechanical Theory of Heat and Probability Calculations Regarding the Conditions for Thermal Equilibrium. Wien. Ber. Vol. 7, pp. 373-435, 1877.

[36]E. Jaynes. Information Theory and Statistical Mechanics. Physical Review, vol. 106, no. 4, pp. 620-630, May 1957.

[37]W. Heisenberg. The Actual Content of Quantum Theoretical Kinematics and Mechanics. Z. Phs., vol. 43, pp. 172, 1927.

Acknowledgments

First of all, we would like to express our deep gratitude to Mr. Sun Changnian. Since 1997, he has provided professor Liang with the opportunity to explore efficient digital modulation methods. He was also the first to support the initial idea of TS-NMT. When the rationality of TS-NMT was proved by simulation, we have been cooperating for a long time since 2005 with the goal of using TS-NMT for xDSL. Mr. Sun Changnian was responsible for the development of hardware prototype and commercial financing. Unfortunately, due to the lack of funds and human resources, we have not been able to enter the business road! However, a prototype for experiment has been made, which helps us to complete the verification of short-distance wired and wireless physical channels. We also thank three doctoral students and 33 master's students from Xi'an Jiaotong University and Dalian Maritime University who have done a lot of computer simulation and physical channel experiments from 1997 to 2010. Funding: This research was supported via the Natural Science Foundation of China (NSFC) (60272017, 60772160). Author contributions: Dequn Liang wrote the first draft and reviewed the final draft. Xinyu Dou completed the computer simulation and editing of the full text mentioned in the article. Competing interests: Dequn Liang is the author of two international patents related to this work (application. no. 00123342.4 and 200810119412.1). Xinyu Dou declares no competing interests. Data and materials availability: All data needed to evaluate the conclusions in the paper are present in the paper. Additional data related to this paper may be requested from the authors.